www.dergipark.gov.tr
ISSN:2148-3736
El-Cezerî Fen ve Mühendislik Dergisi
Cilt: 8, No: 3, 2021 (1243-1253)

El-Cezerî Journal of Science and Engineering
Vol: 8, No: 3, 2021 (1243-1253)
DOI:10.31202/ecjse.909855

ECJSE

Research Paper / Makale

Design and Simulation of a Microchannel Heat Exchanger for Cooling a Micro Processor Using Ethylene

Busra TOM[a], Erhan KAYABASI[b*]

[a]Institute of Science, Mechanical Engineering Department Karabuk University, Karabuk, Turkey
[b]Engineering Faculty, Mechanical Engineering Department, Karabuk University, Karabuk, Turkey
erhankayabasi@karabuk.edu.tr

Received/Geliş: 05.04.2021 **Accepted/Kabul:** 18.06.2021

Abstract: In this study, a microchannel heat exchanger was proposed instead of a conventional air-cooled heat sink in order to obtain uniform surface temperature distribution. In addition, flow and heat transfer simulations were performed using Flo-EFD software. First, the temperature distribution of the air domain and microprocessor in the computer case was obtained. Afterward, the system with the proposed microchannel heat exchanger was subjected to the same processes, and the results were compared. As a result of the study, it was revealed that the microchannel heat exchanger reduced the processor temperature between 54-55 °C and 18-19 °C. It has also been observed that removing the heat sink allows the air drawn from the outside environment to circulate more efficiently around other heat-generating elements in the computer case. Hence, a more homogeneous and lower temperature distribution within the computer case was obtained.

Keywords*:* Liquid cooling, microchannel, heat exchanger, microprocessor, ethylene.

Bir Mikro Işlemcinin Soğutulmasi için Etilen ile Çalışan bir Mikro Kanallı Isı Değiştiricisinin Tasarımı ve Simülasyonu

Öz: Bu çalışmada hava soğutmalı mikroişlemcili ısı emiciler mikrokanallı bir ısı değiştirici önerilmiştir. Flo-EFD yazılımı kullanılarak akış ve ısı transferi simülasyonları yapılmıştır. Öncelikle hava soğutmalı soğutucu için bilgisayar kasasındaki hava havmi ve mikroişlemcinin sıcaklık dağılımı elde edilmiş, ardından fan yardımı ile dışarıdan gelen havanın akış yolları gözlemlenmiştir. Daha sonra önerilen mikrokanallı ısı değiştiricisi kullanılan sistem aynı işlemlere tabi tutulmuş ve sonuçlar karşılaştırılmıştır. Çalışma sonucunda mikrokanallı ısı değiştiricinin işlemci sıcaklığını 54-55 °C'den 18-19 °C'ye düşürdüğü ortaya çıkmıştır. Soğutucunun çıkarılmasının, dış ortamdan çekilen havanın bilgisayar kasasındaki diğer ısı üreten elemanlar etrafında daha verimli bir şekilde dolaşmasına izin verdiği de gözlemlenmiştir. Böylelikle bilgisayar kasası içerisinde daha homojen ve daha düşük sıcaklık dağılımı elde edilmiştir.

Anahtar Kelimeler: Sıvı soğutma, mikrokanal, ısı değiştiricisi, mikroişlemci, etilen.

1. Introduction

Waste heat recovery is a hot topic for many industrial applications such as automotive, iron steel, glass, ventilation and air conditioning, power cycles due to the increase in oil prices on macroeconomic indicators [1–6]. However, some devices also need to be cooled to remain at optimum operating conditions, such as electronic devices and microprocessors. Among them, microprocessors are significant devices for computers to perform several processes in a specific duration. However, microprocessors are dense heat devices up to 300 W/cm^{2,} and they have to be

Bu makaleye atıf yapmak için
Tom, B, Kayabasi, E,*"Bir Mikro Işlemcinin Soğutulmasi için Etilen ile Çalışan bir Mikro Kanallı Isı Değiştiricisinin Tasarımı ve Simülasyonu"* El-Cezerî Fen ve Mühendislik Dergisi 2021, 8 (3); 1243-1253.

How to cite this article
Tom, B, Kayabasi, E "*Design and Simulation of a Microchannel Heat Exchanger for Cooling a Micro Processor Using Ethylene*" El-Cezerî Journal of Science and Engineering, 2021, 8.(3); 1243-1253.
ORCID ID: [a]0000-0001-8219-3069, [b]0000-0002-3603-6211

around 85 °C for maximum performance and showing an increasing temperature profile during the increasing processes [7]. An increase in temperature causes a severe decrease in the process performance due to decreased electrical conductivity of the conductors and semiconductor materials used in microprocessors [8]. The necessity of high heat dissipation in electronic devices made it necessary to design more efficient and reliable cooling systems [9,10]. For the cooling of microprocessors, air cooling systems are intensively applied. In addition, some unique systems are designed to overcome the heating issue in high-temperature levels, such as micro heat exchangers, phase changing materials (PCM) and microchannel heat sinks [8,11].

Microchannel heat exchangers can be applied in the cooling of small volume devices operated under high temperatures such as electrical components [12]. Microchannels, which are essential parts used extensively in micro heat exchangers to enhance heat transfer with a compact application, have a very high surface area/volume ratio and very short heat transfer distance [13,14]. In addition, nanoparticles are a standard application in recent years to increase fluids' cooling performance and the heat flux from targeted heat resources [8,15].

A well-designed micro heat exchanger must receive higher performance from microprocessors to overcome the high-temperature difference issue. For this purpose, many studies were conducted on the effective cooling of microprocessors.

Ariyo and Ochende carried out a micro-sized heat exchanger's constructional design consisting of microchannels [9]. In the study, they optimized the dimensions and flow parameters of two-phased cooling fluid. As a result, it was found that two-phase flow regimes in rectangular microchannels successfully achieved high heat transfer at low Reynolds numbers. Hernando et al. [16] analyzed the fluid flow and heat transfer experimentally using non-phase change liquid, deionized water, a micro heat exchanger. In their study, 100x100 μm and 200x200 μm square cross-section micro-channel heat exchangers were designed. As a result of the small-scale microchannels, the effect of increasing heat transfer or pressure drop was not observed. Yang et al. [17] investigated the thermal performance of gas-gas micro heat exchangers operating under different flows (parallel-flow, counter-flow, cross-flow). Therefore, the double-layer microchannel heat exchanger is designed. Different materials (copper, peek, stainless steel, and aluminum) and various foils of different thicknesses have been investigated to prove the effect of axial fluid conjugate heat transfer on the thermal efficiency of the micro heat exchanger. It was concluded that conjugate heat transfer could be very powerful in micro heat exchangers and shown that countercurrent tends to reduce the efficiency of micro heat exchangers.

In contrast, cross current tends to increase the efficiency of micro heat exchangers. Dondapati et al. [18] calculated pressure drops and heat transfer rate in a micro heat exchanger. They were operated the microchannel heat exchanger with cryogen-based nanofluids. They observed that the thermal conductivity of the nanofluid increases with the increase in the volume concentration of the nanoparticles. With this, the heat transfer rate of the micro heat exchanger increases. Liquid nitrogen as base liquid and CuO, SiO_2, SiC, Al_2O_3 and TiO as nanoparticles were considered. The decrease in pressure drop with CuO nanoparticle suspension as a cryogen-based nanofluid was found to be small.

Furthermore, it was observed that heat transfer increased with a concentration of 3% by volume of Al_2O_3 and SiO_2 nanoparticles. Kang and Tseng [19] analyzed efficiency and pressure drop in a cross-flow heat exchanger and developed a theoretical model micro heat exchanger. According to the analytical results, the average temperature of the hot and cold flow significantly affected the heat transfer rate and pressure drop under identical operating effectiveness. It provides 148 kW thermal conductivity when silicon is used in micro heat exchanger construction and 400 kW thermal

conductivity when copper is used, but the heat exchanger efficiency is similar. The dimensions have a significant effect on the relationship between the heat transfer rate and the pressure drop. Marcinichen et al. [20] have designed three micro-evaporator cooling cycles to cool a computer's microprocessor. Four different refrigerants were used as working fluids to remove heat from the microprocessor, and HFC134a and HFC245fa achieved the most efficient results. Jajja et al. [21] have examined flat plate heat sinks at intervals of 0.2 mm, 0.5 mm, 1.0 mm, and 1.5 mm for efficient thermal management of microprocessors that produce high heat. By reducing the fin spacing and increasing the volumetric flow rate of the circulating water in the heat sink, the heat sinks' base temperature and thermal resistance are reduced. For a flat plate heat sink, the maximum thermal resistance was reduced from 0.216 K/W to 0.03 K/W using a heat sink of 0.2 mm fin spacing. The total heat transfer coefficient increased twice.

In this context, this study aims to remove the heat from the overheated microprocessor with a microchannel heat exchanger using ethylene and compare it with the air-cooled system. First, the air domain's temperature distribution and the microprocessor's surface in the computer case were obtained by flow and heat transfer simulations with an air-cooled heat sink. The flow paths of the air coming from the outside with the help of the fan were observed. Afterward, the system with the proposed microchannel heat exchanger was subjected to the same processes, and the results were compared.

2. Materials and Methods

In this study, two distinguished cooling case studies were simulated using Flo-EFD simulation software developed by Simcenter for a sample computer case consisted of one microprocessor, one power supply, three transistors, and eight ram units that dissipating heat. The enclosure volume was cooled with a fan, and an aluminum heat sink mounted on the 50 mmx50 mmx1.2 mm dimensioned plate in the initial case. In the second case, a micro pipe heat exchanger made of copper in 0.82 mm using ethylene as coolant liquid was mounted on the microprocessor instead of the heat sink, as shown in Figure 1. Coolant velocities are varied between 0.1 m/s and 1.02 m/s and the diameters of the channel are varied between 0.32 mm to 0.9 mm [18,19,22]. The inlet velocity of ethylene and the microchannel diameter are set to 0.5 m/s and 0.82 mm by inspiration from the previous studies.

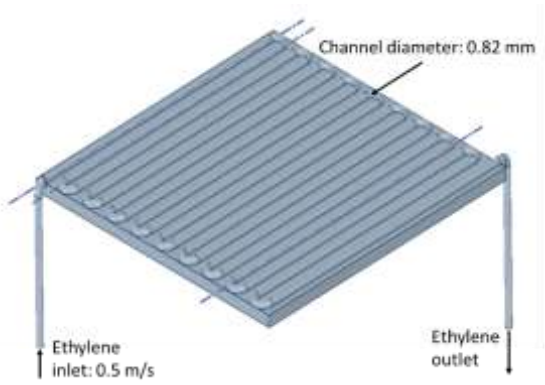

Figure 1. Microchannel heat exchanger for the microprocessor.

The microchannels were semi-submerged into 0.41 mm 50mmx50mmx1.2mm dimension plates to benefit from the heat convection of surrounding air in the case. Cooling operation for the case studies was demonstrated schematically in Figure 2. To understand the effects of cooling options, temperature distribution and flow paths were observed both in the enclosure volume and on the microprocessor.

In this study, heat dissipations were selected identical for the two cooling options as 10 W for microprocessor, 20 W for power supply, 1 W per ram unit (total 8 W). In addition, 80 °C surface temperature is given as a constant temperature boundary condition for the transistors. The fan type was selected identic for both studies from the software library as Axial Papst 412 H, and the ambient air temperature was set to 25 °C. The pressure of the surrounding air was set to 101 kPa. The coolant velocity in the microchannel heat exchanger was set to 0.5 m/s. For accurate results, a sufficient mesh density is mandatory. For this purpose, the heat sink, microchannel heat exchanger and the surrounding air were meshed separately to meet the details in geometries.

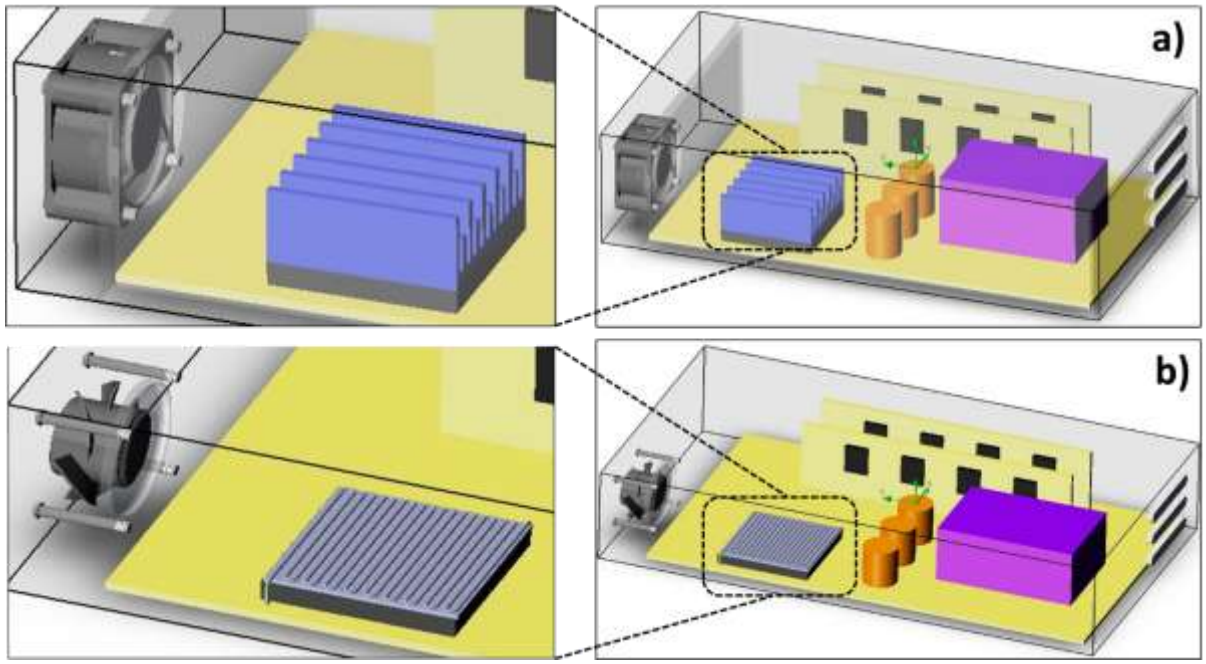

Figure 2. General arrangements of cooling options: a) with heat sink, b) with microchannel heat exchanger.

Flo-EFD software was employed in CFD simulation to observe the temperature distribution on the microprocessor with heat sink and microchannel heat exchanger separately. Flo-EFD solves conservation equations for mass, momentum, and energy. The equation for conservation of mass, or continuity equation, can be written as follows:

$$\frac{\partial \rho}{\partial t} + \nabla \cdot (\rho \vec{v}) = S_m \tag{1}$$

The equation is the generalized shape of the mass conservation definition, and s is used for incompressible and compressible flows. Mass of flow put to the continuous phase from the dispersed second phase (e.g., due to vaporization of liquid droplets) and any user-defined sources. The conversation of energy definition is given in Equation (2);

$$\left(u\frac{\partial T}{\partial x} + v\frac{\partial T}{\partial y} + w\frac{\partial T}{\partial z}\right) = \alpha\left(u\frac{\partial^2 T}{\partial x^2} + v\frac{\partial^2 T}{\partial y^2} + w\frac{\partial^2 T}{\partial z^2}\right) \tag{2}$$

Here, *u*, *v* and *w* are velocity components in the directions of *x*, *y*, *z*, respectively, and α is the thermal emission coefficient. Conservation of momentum in an inertial reference frame is given by:

$$\frac{\partial}{\partial t}(\rho \vec{v}) + \nabla \cdot (\rho \vec{v}\vec{v}) = \nabla p + \nabla \cdot (\bar{\bar{\tau}}) + \rho g + \vec{F} \tag{3}$$

where p is the static pressure, $\bar{\bar{\tau}}$ is the stress tensor, and ρg and F are the gravitational body force and external body forces, respectively. $\vec{F}$ also includes other model-dependent source terms such as porous-media and user-defined sources. The stress tensor was calculated with Equation (4).

$$\bar{\bar{\tau}} = \mu\left[(\nabla\vec{v} + \nabla\vec{v}^T) - \frac{2}{3}\nabla\cdot\vec{v}I\right] \quad (4)$$

Here μ is the molecular viscosity, I is the unit tensor, and the second term on the right is the effect of volume dilation. Reynolds number was calculated by Equation (5) for the flows in channels.

$$Re_D = \frac{\rho u_m D}{\mu} \quad (5)$$

Here ρ is the density of air, u_m is mean velocity of air in the channel, D is the diameter of channel, μ is the dynamic viscosity of ethylene at 300 K.

3. Results and Discussions

Two different simulations were made to examine the temperature distribution on the air domain and microprocessor in the computer case. Figure 3 shows the temperatures on the heat sink and the processor for the heat sink option. Accordingly, it is observed that the lowest temperature on the processor is 54.91 °C, and the highest temperature is 55.42 °C. In addition, it is observed that the temperature increases as it moves away from the fan zone. Similarly, it is observed that the lowest temperature is 54.65 °C, and the highest temperature is 55.28 °C on the heat sink.

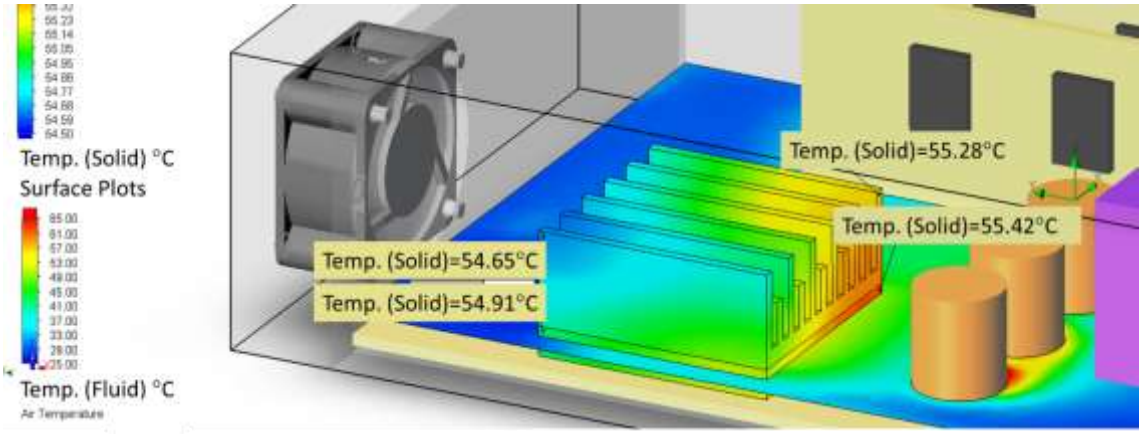

Figure 3. Temperature distribution of microprocessor and heat sink.

Temperature distributions can be examined in Figure 4 when microchannel heat exchangers are used under the same conditions. Accordingly, it is observed that the temperature values are at much lower levels compared to the situation where the heat sink is used. For example, the lowest and highest temperatures on the microprocessor were observed as 18.53 °C 19.74 °C at the inlet and outlet of the coolant to the heat exchanger, respectively. Thus, despite having the highest temperature difference of 1.21 °C on the microprocessor, the average operating temperature values were obtained at approximately 26 °C lower than the option using the heat sink.

The airflow paths and overall temperature distributions in the computer case are given in Figure 5 and Figure 6 for the option with the heat sink microchannel heat exchanger, respectively. According to Figure 5, it was observed that the air domain is around 50-55 °C in the upper right region of the heat sink. Temperature distribution around the power supply has been achieved relatively low, around 25-35 °C. Similarly, it is observed that the air temperature around the microchips is 50-55 °C. However, it is seen that the temperature around the capacitors exceeds 65 °C. In addition, it is

observed that the density of flow vectors decreases in regions with high-temperature values. In addition, the high-temperature values on the capacitors indicate that the geometry of the heat sink makes it difficult for the flow to reach the capacitor region.

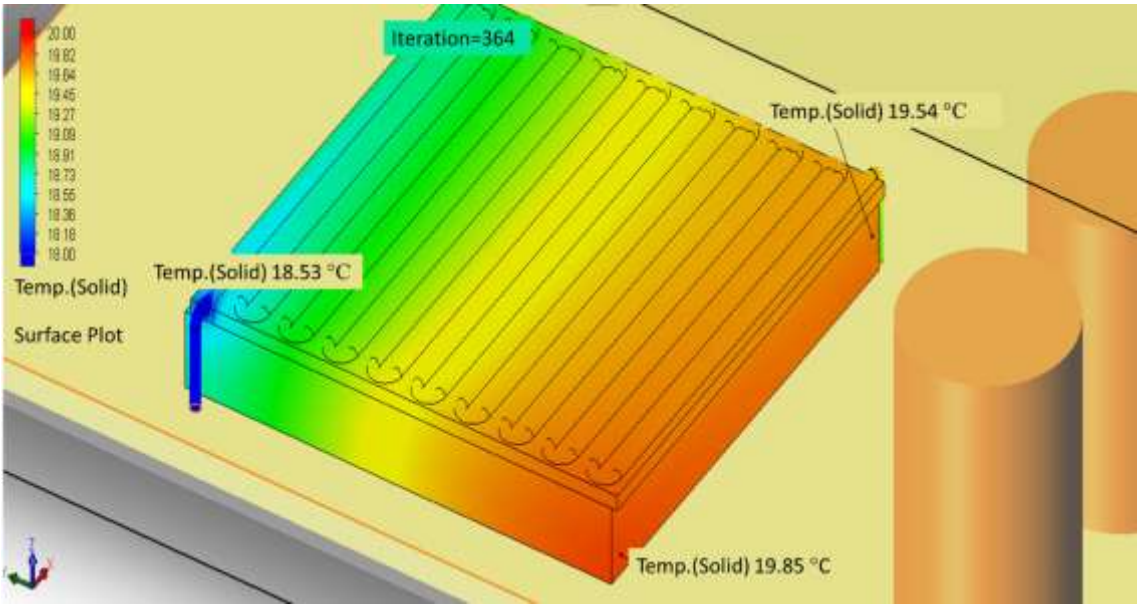

Figure 4. Temperature distribution of the microprocessor and microchannel heat exchanger.

On the contrary, it is observed that the cold airflow coming through the fan hits the heat sink and directs to areas where there are no heat-generating elements. Thus, while the heat sink provides a weak cooling for the microprocessor, it also prevents the cooling of other heat-generating components in the case.

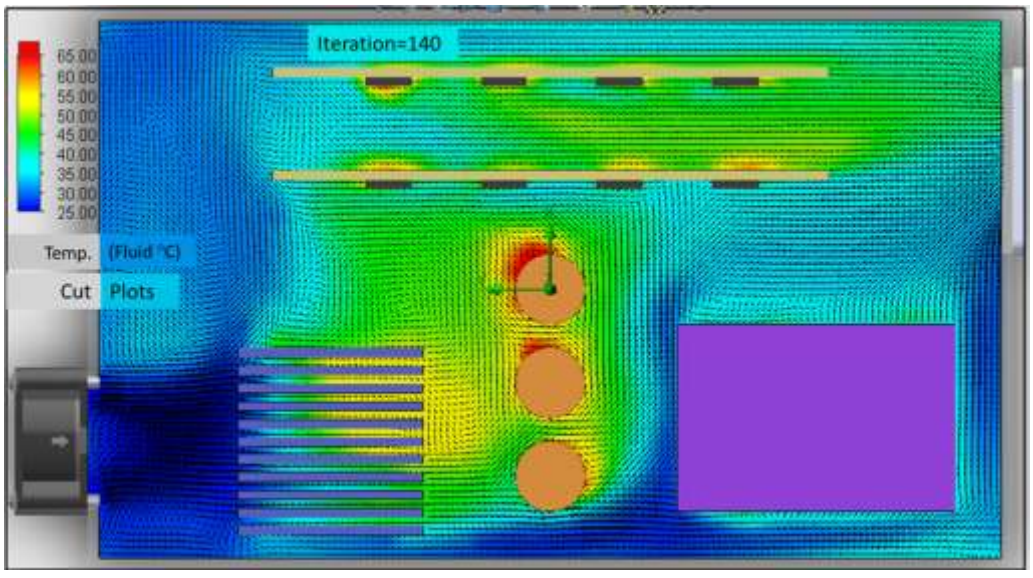

Figure 5. Flow path and temperature distribution of air domain in the computer case with the heat sink.

Figure 6 shows that the air domain in the computer casing is at lower levels than the heat sink option. It is observed that the temperature of the air circulating the microprocessor is around 25 °C. Similarly, the air domain around the capacitors was observed at approximately 25-30 °C and about 42-53 °C on the back surfaces. In addition, it is seen that the air temperature around the power

supply is maintained at around 30 °C. The microchips' temperatures could be kept at about 30 °C since the air came directly to microchips at the first row after the heat exchanger. However, the temperature of the air coming to the remaining microchips was obtained around 50 °C.

When the flow vectors are examined, the airflow successfully circulates the region of the microprocessor, power supply, capacitors and microchips. However, it is observed that the air circulation around the microchips in the rear area is weaker than in the first row. This situation also supports the temperature increase in this region.

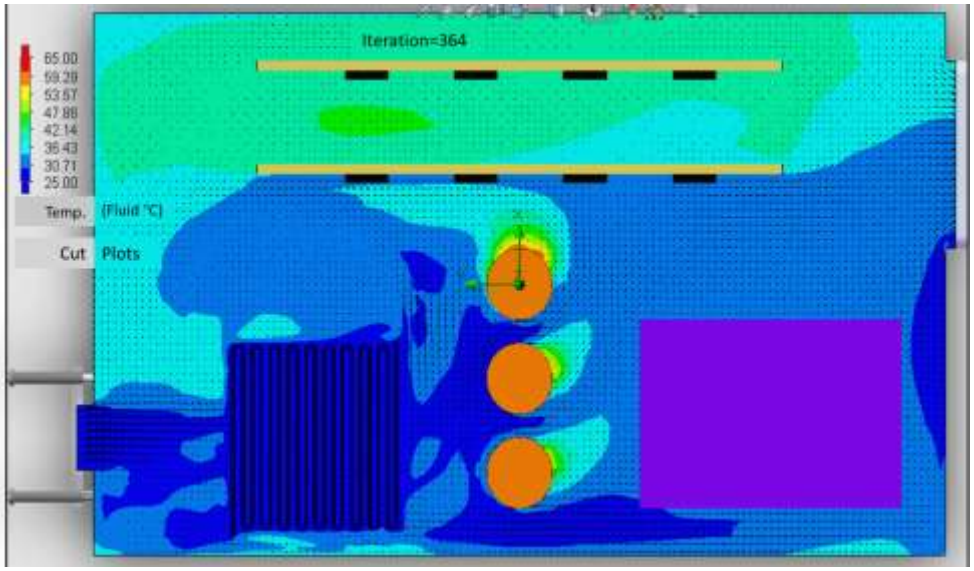

Figure 6. Flow path and temperature distribution of air domain in the computer case with heat exchanger.

Figures 7 and 8 show at what rates the heat generated in the processor is transferred to which elements. According to Figure 7, 8.68 W of the 10 W generated by the microprocessor was transferred directly to the heat sink. The heat sink transferred more heat to the air domain than it received from the microprocessor. The remaining heat is also absorbed from other elements, primarily capacitors, near the heat sink and transferred to the air.

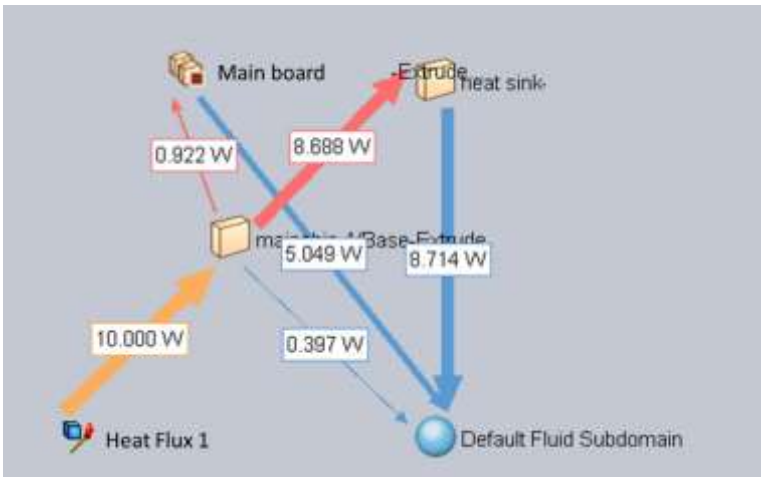

Figure 7. Heat flux diagram for the heat sink.

In addition, the microprocessor transferred 0.922 W directly to the shell of the case and 0.397 W directly to the air from the surfaces where the heat sink is not in contact. According to Figure 8, 10.5 W was transferred directly to the heat exchanger. In addition, the heat exchanger was exposed to about 1 W of heat by the air domain.

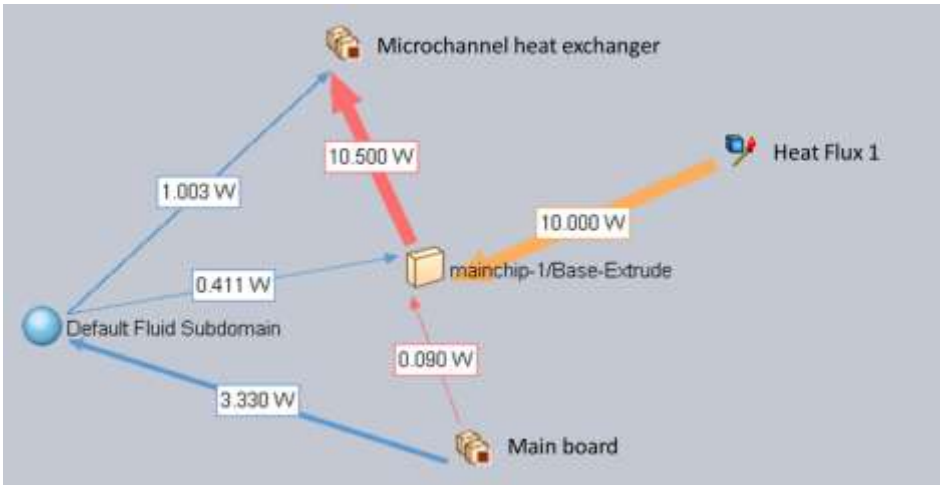

Figure 8. Heat flux diagram for microchannel heat exchanger.

Similarly, due to the low temperature resulting from the successful cooling of the heat exchanger, the air also heated the microprocessor by 0.411 W by conduction heat transfer instead of cooling it. Finally, 3.330 W of heat transfer by conduction from the inner shell of the computer case to the air domain and 0.09 W to the microprocessor were realized by convection heat transfer. As a result, while the micro-channel heat exchanger successfully cools the microprocessor, some heat flow has occurred from the shell of the computer case to the microprocessor from the interior air. While the microprocessor, which produces high heat under normal conditions, is expected to be cooled by the air domain, the micro-channel heat exchanger placed on the processor has succeeded in keeping the processor temperature below the temperature of the ambient air and surrounding elements. Overall heat transfer coefficient variations in X and Y direction on the microchannel heat exchanger were supplied in Figure 9. According to Figure 9a, the overall heat transfer coefficient varied from 2 W/m^{2}K to 70 W/m^{2}K by the length of X-direction. In addition, the overall heat transfer coefficient ranged from 77 W/m^{2}K up to 300 W/m^{2}K by the length of the Y direction.

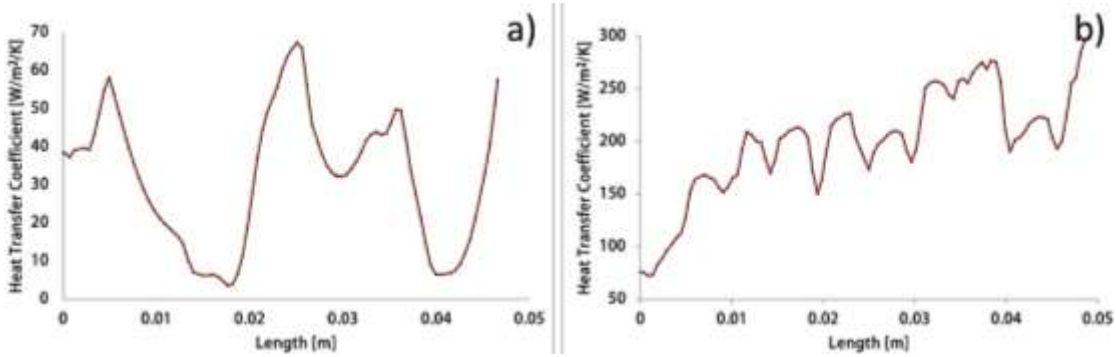

Figure 9. Overall heat transfer coefficient for microchannel heat exchanger: a) X direction, b) Y direction.

Overall heat transfer coefficient variations in X and Y direction on the heat sink were supplied in Figure 10. According to Figure 10a, the overall heat transfer coefficient varied from 17 W/m^{2}K up to 20 W/m^{2}K by the length of X-direction. In addition, the overall heat transfer coefficient ranged

from 1 W/m^{2}K up to 29 W/m^{2}K by the length of the Y direction. It is clearly observed in the overall heat transfer coefficients curves of both applications, the microchannel is showing promising performances in both directions X and Y on the microprocessor.

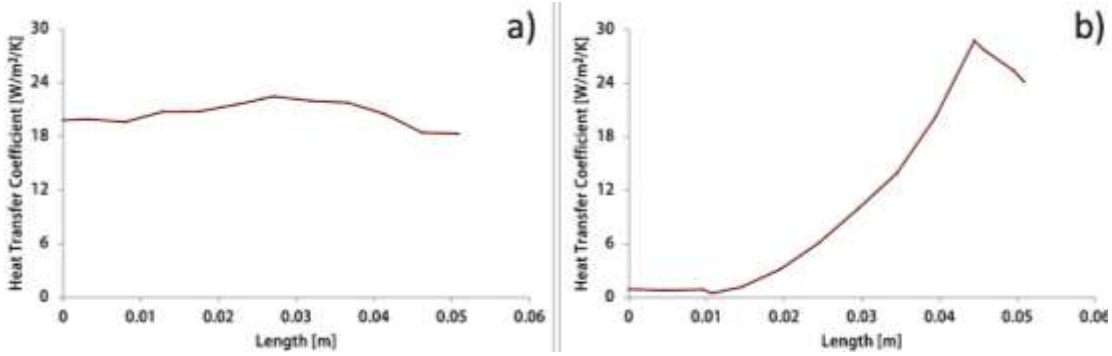

Figure 10. Heat transfer coefficient for heat sink: a) X direction, b) Y direction.

4. Conclusions

A microchannel heat exchanger operating with ethylene was proposed in this study instead of conventionally used microprocessor heat sinks. Flow and heat transfer simulations were performed using Flo-EFD software. As a result of the study;

- It was revealed that the microchannel heat exchanger could keep the processor temperature around 18-19 °C instead of 54-55 °C.
- In this study, a microchannel heat exchanger was proposed instead of a conventional air-cooled heat sink in order to obtain uniform surface temperature distribution.
- It has been observed that the removal of the heat sink allows the air drawn from the outside environment to circulate more efficiently around other heat-generating elements in the computer case, allowing a more homogeneous and lower temperature distribution inside the computer case.
- This study should be extended by working parametrically to optimize heat exchanger microchannels and determine the type and flow rates of the fluids in the heat exchanger.
- For future studies, experimental validation is planned to determine the optimum operating conditions to provide uniform temperature distribution on microprocessors.

Acknowledgment

We are grateful to Karabuk University for providing its software and hardware infrastructure to realize the current study.

'Authors' Contributions

EK performed general conceptualization, investigation, review, and final checking of the study. BT has performed simulation studies and realized writing and original drafts.

Both authors read and approved the final version of the article.

Competing Interests:

The authors declare that they have no conflict of interest.

References

[1]. Kunt MA. İçten Yanmalı Motor Atık Isılarının Geri Kazanımında Termoelektrik Jeneratörlerin Kullanımı. El-Cezeri Fen ve Mühendislik Dergisi, 2016, 3:192–203. doi:10.31202/ecjse.264183.

[2]. Akçay H, Gürbüz H, Demirtürk S, Topalcı Ü. Tipik Bir Buji Ateşlemeli Motorda Egzoz Atık Isısı Enerjisinin Geri Kazanımı İçin Geliştirilen Termoelektrik Jeneratörün HAD Analizi. El-Cezeri Fen ve Mühendislik Dergisi, 2020, 1088–100. doi:10.31202/ecjse.724353.

[3]. Akyürek Z. Energy Recovery and Greenhouse Gas Emission Reduction Potential of Bio-Waste in the Mediterranean Region of Turkey. El-Cezeri Fen ve Mühendislik Dergisi, 2019. doi:10.31202/ecjse.551780.

[4]. Ozcan H, Kayabasi E. Thermodynamic and economic analysis of a synthetic fuel production plant via CO2 hydrogenation using waste heat from an iron-steel facility. Energy Convers and Manag, 2021, 236:114074. doi:10.1016/j.enconman.2021.114074.

[5]. Kayabasi E, Alperen MA, Kurt H. The effects of component dimensions on heat transfer and pressure loss in shell and tube heat exchangers. Int J Green Energy, 2019, 16:200–10. doi:10.1080/15435075.2018.1555162.

[6]. Mugaloglu E, Polat AY, Tekin H, Dogan A. Oil Price Shocks During the COVID-19 Pandemic : Evidence From United Kingdom Energy Stocks, 2021, 2:1–5.

[7]. Cheng L, Thome JR. Cooling of microprocessors using flow boiling of CO2 in a micro-evaporator: Preliminary analysis and performance comparison. Appl Therm Eng 2009;29:2426–32. doi:10.1016/j.applthermaleng.2008.12.019.

[8]. Hatami M, Ganji DD. Thermal and flow analysis of microchannel heat sink (MCHS) cooled by Cu-water nanofluid using porous media approach and least square method. Energy Convers Manag, 2014;78:347–58. doi:10.1016/j.enconman.2013.10.063.

[9]. Ariyo DO, Bello-Ochende T. Constructal design of subcooled microchannel heat exchangers. Int J Heat Mass Transf, 2020, 146:118835. doi:10.1016/j.ijheatmasstransfer.2019.118835.

[10]. Devahdhanush VS, Lei Y, Chen Z, Mudawar I. Assessing advantages and disadvantages of macro- and micro-channel flow boiling for high-heat-flux thermal management using computational and theoretical/empirical methods. Int J Heat Mass Transf, 2021, 169:120787. doi:10.1016/j.ijheatmasstransfer.2020.120787.

[11]. Ghazvini M, Shokouhmand H. Investigation of a nanofluid-cooled microchannel heat sink using Fin and porous media approaches. Energy Convers Manag, 2009, 50:2373–80. doi:10.1016/j.enconman.2009.05.021.

[12]. Sai Suhruth Teja K. Optimization of parameters and fabrication of micro channel heat sinks using micro scanning EDM and grey relational analysis. Mater Today Proc, 2021. doi:10.1016/j.matpr.2020.12.951.

[13]. Gerken I, Brandner JJ, Dittmeyer R. Heat transfer enhancement with gas-to-gas micro heat exchangers. Appl Therm Eng, 2016, 93:1410–6. doi:10.1016/j.applthermaleng.2015.08.098.

[14]. Deng Y, Menon S, Lavrich Z, Wang H, Hagen CL. Design, simulation, and testing of a novel micro-channel heat exchanger for natural gas cooling in automotive applications. Appl Therm Eng, 2017,110:327–34. doi:10.1016/j.applthermaleng.2016.08.193.

[15]. Maganti LS, Dhar P, Sundararajan T, Das SK. Heat spreader with parallel microchannel configurations employing nanofluids for near–active cooling of MEMS. Int J Heat Mass Transf, 2017, 111:570–81. doi:10.1016/j.ijheatmasstransfer.2017.04.032.

[16]. García-Hernando N, Acosta-Iborra A, Ruiz-Rivas U, Izquierdo M. Experimental investigation of fluid flow and heat transfer in a single-phase liquid flow micro-heat exchanger. Int J Heat Mass Transf, 2009, 52:5433–46. doi:10.1016/j.ijheatmasstransfer.2009.06.034.

[17]. Yang Y, Morini GL, Brandner JJ. Experimental analysis of the influence of wall axial conduction on gas-to-gas micro heat exchanger effectiveness. Int J Heat Mass Transf, 2014, 69:17–25. doi:10.1016/j.ijheatmasstransfer.2013.10.008.

[18]. Dondapati RS, Saini V, Verma KN, Usurumarti PR. Computational prediction of pressure drop and heat transfer with cryogen based nanofluids to be used in micro-heat exchangers. Int J Mech Sci, 2017, 130:133–42. doi:10.1016/j.ijmecsci.2017.06.012.
[19]. Kang SW, Tseng SC. Analysis of effectiveness and pressure drop in micro cross-flow heat exchanger. Appl Therm Eng, 2007, 27:877–85. doi:10.1016/j.applthermaleng.2006.09.002.
[20]. Marcinichen JB, Thome JR, Michel B. Cooling of microprocessors with micro-evaporation: A novel two-phase cooling cycle. Int J Refrig, 2010, 33:1264–76. doi:10.1016/j.ijrefrig.2010.06.008.
[21]. Jajja SA, Ali W, Ali HM, Ali AM. Water cooled minichannel heat sinks for microprocessor cooling: Effect of fin spacing. Appl Therm Eng, 2014, 64:76–82. doi:10.1016/j.applthermaleng.2013.12.007.
[22]. Farisè S, Franzoni A, Poesio P, Beretta GP. Heat transfer enhancement by spinodal decomposition in micro heat exchangers. Exp Therm Fluid Sci, 2012, 42:38–45. doi:10.1016/j.expthermflusci.2012.03.024.